NANOSYSTEMS: PHYSICS, CHEMISTRY, MATHEMATICS, 2018, 9 (5), P. 603–608

Flintstone as a nanocomposite material for photonics

P. P. Fedorov[1], V. A. Maslov[1], V. V. Voronov[1], E. V. Chernova[1], O. S. Kudryavtsev[1], V. G. Ralchenko[1], I. I. Vlasov[1], A. S. Chislov[1], M. N. Mayakova[1], E. G. Yarotskaya[1], R.V. Gaynutdinov[2], P. A. Popov[3], A. I. Zentsova[3]

[1]Prokhorov General Physics Institute of the Russian Academy of Sciences, 38 Vavilov Street, Moscow, 119991 Russia

[2]Crystallography and Photonics Federal Research Center, Russian Academy of Sciences, 59 Leninskii Prospect, Moscow, 119991 Russia

[3]Petrovskii State University, 14 Bezhitskaya Street, Bryansk, 241036 Russia

ppfedorov@yandex.ru

DOI 10.17586/2220-8054-2018-9-5-603-608

Studying natural flintstone samples' properties, including optical transparency and thermal conductivity, by various physical methods (X-ray diffraction, atomic force microscopy, optical microscopy, etc.) revealed that said specimens contain chalcedony nanoparticles bund into the complex hierarchial structure.

Keywords: flintstone, quartz, chalcedony, thermal conductivity, nanocomposite, nanographite photonics.

Received: 17 September 2018

Revised: 26 September 2018

1. Introduction

Recently, significant progress has been made in the manufacturing of various nanophotonic structures with novel optical properties. Photonic crystals possess ordered distribution of identical elements making up said structures. Usually, such elements are considered monodispersed with regard to their geometric and dielectric parameters; and such materials properties are determined by the whole particle ensembles [1]. In contrast with the latter materials, there are other objects previously described in the literature which consist of disorderly arranged particles. The latter objects can also generate so-called random lasing, and such lasing opens enormous opportunities in miniaturizing laser devices [2–5]. Media with disorderly distributed particles can contain particles of the same or different sizes (i.e., photonic glasses and/or Levy glasses, respectively). Photonic glass properties, in contrast with photonic crystals, are determined by the individual properties of the scattering elements. Such features provide photonic glasses with unique properties and allow novel venues for light propagation in disordered media [2–5],whereas photon transfer in Levy glasses is determined by Levy statistics.

Precipitation of fluoride and oxide nanopowders from aqueous solutions produced unusual monolithic optically transparent precipitates that consisted of agglomerated nanopowders and aqueous solutions binding said nanoparticles together; such precipitates were named as transparent compacts [6–12]. As per our data [6–12], such ability to form these transparent compacts is independent from the nature of the forming nanoparticles: transparent compacts have been obtained for numerous fluorite- and tysonite-type phases (cubic and trigonal systems, respectively) as well as for oxide precursors of aluminum-yttrium garnets and aluminum-magnesium spinels.

Formation of the above materials proceeded via various multistep agglomerations that were very typical for nanotechnology [13–15]. Such processes, which were performed under laboratory conditions, are quite common under natural conditions, too, and one can easily observe their results in the natural formations like quartz minerals, such as chalcedonies, agates, and opals [16–20]. A common feature of these minerals is the presence of small crystalline quartz particles and certain amount of water in them. Opals are characterized by an ordered distribution of spherical silica particles of micron size; and chalcedonies, in general, contain disorderly distributed particles and lower water contenet than other quartz minerals. Flintstones, in turn, are characterized by their various contaminants.

We focused our present work on studying natural flintstones by physical and chemical methods in order to clarify its structure and determine whether flintstone's natural properties were the same as those of laboratory-synthesized samples. We chose black flintstone specimens from the vicinity of Tarusa, Russia, since such flintstones have been widely used for human toolmaking in the Upper Paleolithic and Neolithic Ages and for the manufacture of musket flints in the 18^{th} century.

2. Experimental

Investigated samples were prepared as 0.8 mm thick plates cut out from natural flintstone and thoroughly polished. These specimens were used for X-ray diffraction study, optical transmittance spectra recording and microhardness measurements.

Optical transmittance spectra were recorded with a Carry 5000 spectrometer.

Mineralogical thin sections were used for the sample optical characterization (POLAM L-213 microscope, LOMO, St. Petersburg).

Specimen microhardness was tested using a PRECIDUR DM-8 device under 50 g weight load.

X-Ray diffraction patters were recorded with the use of Bruker D8 Advanced diffractometer (Cu Kα irradiation); obtained data were processed by TOPAS software package; and coherent scattering domain sizes were estimated by Selyakov–Sherer equation: $D = 0.9 \cdot \lambda / B \cdot \cos\theta$, where λ is an X-ray irradiation wavelength, B is an integral peak width, θ is a peak reflection angle.

Surface relief was studied using the scanning probe microscope Ntegra Prima (NT-MDT Spectrum Instruments, Russia) in the contact mode. Employed silicon cantilevers HA_C lever A (Tipsnano, Estonia) are characterized by the following parameters: resonance frequency $f \sim 37$ kHz, tip radius $R \sim 10$ nm, and stiffness constant $k \sim 0.65$ N/m. All experiments on the precision study of the samples surface were carried out under controlled conditions of the TRACKPORE ROOM-05 measuring complex (5 ISO (100) class, humidity of 40 rel. %$\pm$1% and temperature of 24 ± 0.05 °C).

The thermal conductivity of the specimens was measured by the absolute stationary technique of longitudinal thermal flux [21] from 50 – 300 K. Thermal conductivity coefficient values were calculated by Fourier equation within ± 5 % error interval. In the high temperature region 323 – 573 K, thermal conductivity was measured by the dynamic method on an ITλ-400 facility accurate to ± 10 %.

Luminescence and Raman spectra were recorded using confocal HORIBA Jobin Yvon HR800 spectrometer (473 nm wavelength, 10 mW excitation radiation of CIEL Quantum Laser focused by X50 lens to form a 2 micron spot on the sample specimens). For the latter study, we used cleavage faces without any trace of mechanical treatment.

3. Results and Discussion

In our studies, we have used the specimens of dense monolithic appearance with volume about a few cubic centimeters and flinty fractures (1044 $\pm$ 19 kg/mm^2 microhardness; 2.68 g/cm^3 density). A typical X-Ray diffraction pattern for the flintstone samples (Fig. 1) did not change its appearance when taken from monolithic plates or flintstone powder ground in the sapphire mortar.

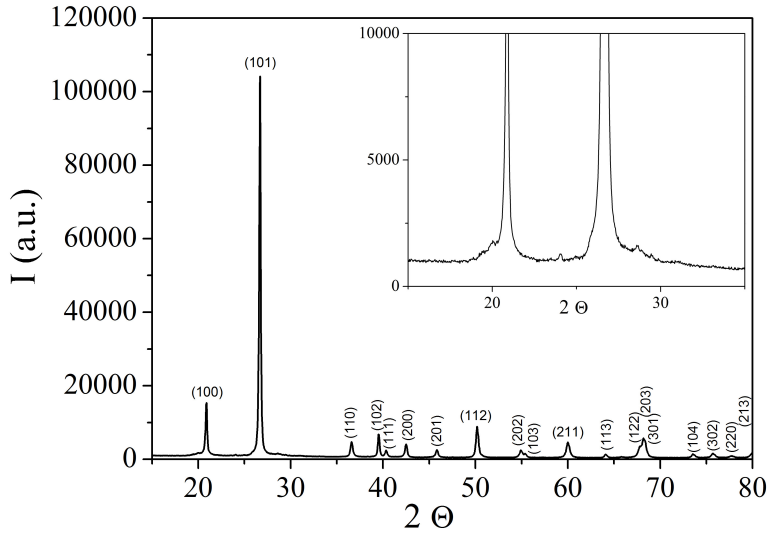

FIG. 1. X-ray diffraction pattern of flintstone specimen

A flintstone diffraction pattern coincides with well-known pattern for alpha-quartz (hexagonal system; $a = 4.913$, $c = 5.405$ Å). Extremely weak reflections at about 20 – 30 2θ degrees (Fig. 1) may be attributed to the rare silica

modification known as moganite (JCPDS card 079-2403). Considering the specimen black color, one may suggest the presence of graphite in the samples masked by overlapping (101) quartz line and the strongest reflection line of said graphite. It is worth noting that flintstone sample reflection lines exhibited different intensities compared to the standard data for alpha-quartz: I_{110}/I_{102} and I_{102}/I_{111} intensity ratios were 0.62 and 4.0, respectively. Such type of the texture has indicated that, according to the known criteria, silica-forming mineral should be characterized as chalcedony [20].

Sizes of the coherent scattering domains D, estimated with the use of the data for (112) and (211) lines, were 31 and 24 nm, respectively.

Atomic force microscopy data for the fresh cleavage face are presented in Fig. 2. They unequivocally confirmed the presence of round-shaped particles (ca. 0.5 microns diameter) in the three-dimensional flintstone framework. One can also see clearly cavities/channels with ca. 2 microns cross-sections in the bodies of said flintstone specimens (Fig. 2).

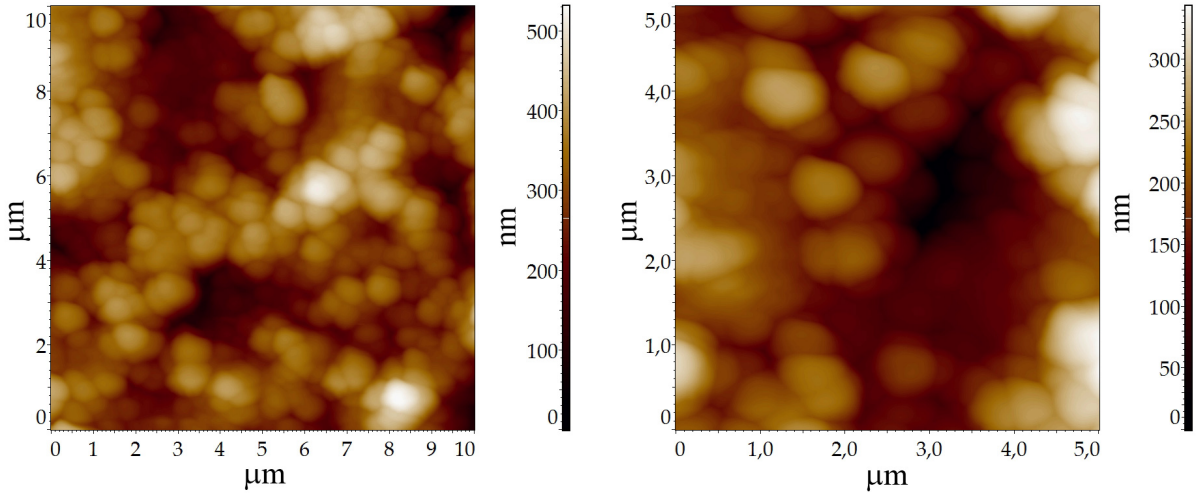

FIG. 2. Atomic Force Microscopy images for flintstone fresh cleavage faces

A typical optical microscopy image of the flintstone mineralogical slide is presented in Fig. 3. Black and white areas with typical size about 10 microns in the said image corresponded to the crystal areas of various orientations: lightening and darkening of each individual area in the slide occurred gradually when the samples were rotated.

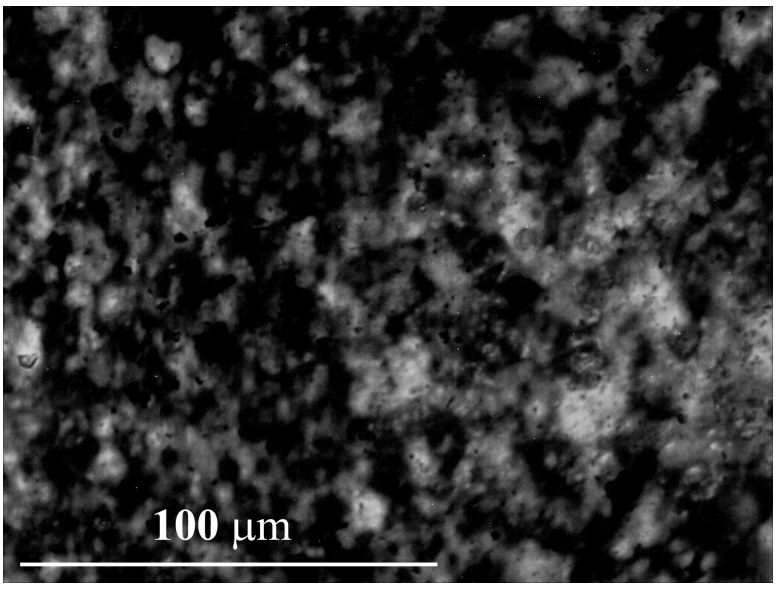

FIG. 3. Optical microscopy image (crossed polarizers)

Analysis of the above data from X-ray diffraction, atomic force microscopy and optical microscopy studies allowed us to conclude that the flintstone structure has several hierarchical levels of organization: nanoparticles with their size of about 30 nm formed round-shaped agglomerates with about 500 nm diameter containing about 5,000 – 10,000 the former 30 nm particles. In turn, the secondary 500 nm nanoparticles formed an easily visible framework in Fig. 2. Comparison of data in Figs. 2 and 3 indicated that merge of the secondary nanoparticles had an oriented crystallographic character (i.e., they intergrew in the right crystallographic orientation), so the whole volume of the flintstone specimen in Fig. 3 was made up of strangely intertwined branched crystal clots.

Despite the black coloration of the studied flintstone specimens, they could be transparent when relatively thin, so their optical transmittance spectra could be recorded (Fig. 4).

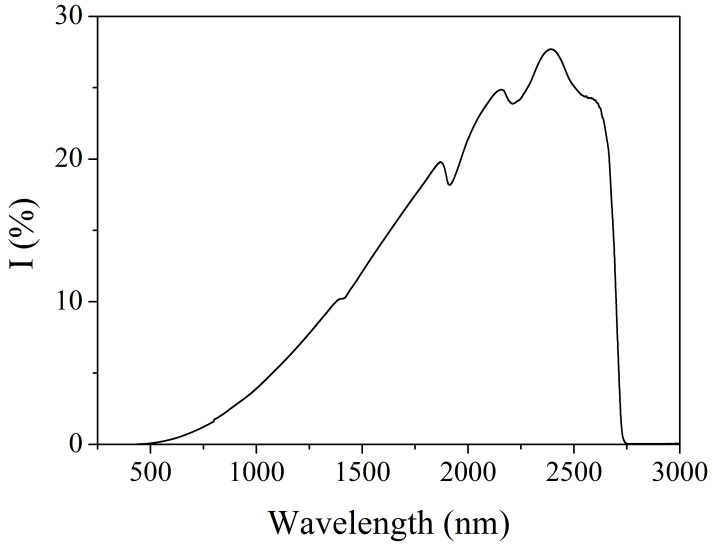

FIG. 4. Optical transmittance spectrum of the 0.8 mm thick flintstone specimen

Flintstone spectra exhibited absorption bands at about 1420, 1920 and 2250 nm wavelengths. The absorption at ∼2180 to 2380 nm has been interpreted as a combination effect of silanol group (Si–OH) and siloxane (Si–O–Si) vibrations. The absorption from 1900 to 2060 nm has been related to the sum of the OH modes in molecular water. The absorption in 1420 nm area was an overtone of OH vibrational modes [22].

Heating flintstone samples under air at 1,000 °C for 1 hour resulted in their discoloration (samples became white) and mass loss of 0.98 wt.%. This might have been related to elimination of the water and previously-mentioned carbon micro-impurities (said carbon might have organic origins). Whereas lines of carbon polymorphs could not be clearly observed in the X-ray diffraction patterns, micro-Raman scattering has been used to determine the presence of carbon and possible types of its inclusions.

The Raman spectrum of the thermally-untreated flintstone specimen (confocal HORIBA spectrometer; Fig. 5) contained one intensive broad line and two weak lines at about 1.400 and 1.600 cm^{-1}. Such lines are typical for Raman scattering of nanographite; the latter lines have been labeled as D and G lines [23], and the former line corresponded to nanocarbon luminescence [24] (Fig. 5 data represent Raman spectrum of flintstone after luminescence component subtraction).

Results of thermal conductivity measurements for various materials are presented in Fig. 6. The data presented unequivocally indicate that the thermal conductivity for flintstone is relatively low and could be placed between the thermal conductivities of single quartz crystals and amorphous quartz glass. Compared to the quartz single crystal data, maximum of the thermal conductivity temperature correlation moved to the higher temperature range, but decreased almost by three orders of magnitude. The same phenomenon has been observed for the disordered crystalline media including $M_{1-x}R_xF_{2+x}$ fluorite-type solid solutions (M = Ca, Sr, Ba; R = rare earth elements) [29].

As we have previously mentioned, flintstone samples are composite materials with complex hierarchic structures. The latter is in complete agreement with literature data: “Thin sections exhibit structure of at least two levels, the larger one of quartz or chalcedony grains ordered aggregates of 1–50 μm size and the smaller grains, combined conformally, that fill in available spaces and have web-toed or amoeboid shapes chalcedony grains are not single crystals, and they fade in a narrow-wave, hand-fan or cross-type style, in contrast with quartz crystals.

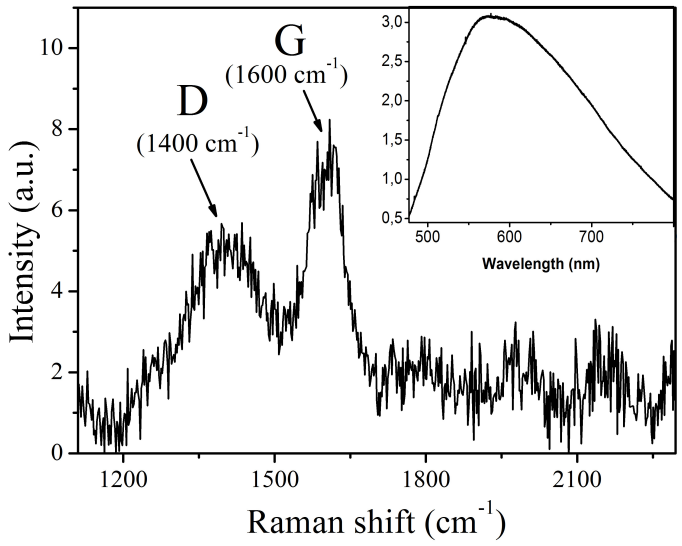

FIG. 5. Raman spectrum of flintstone sample after luminescence component subtraction

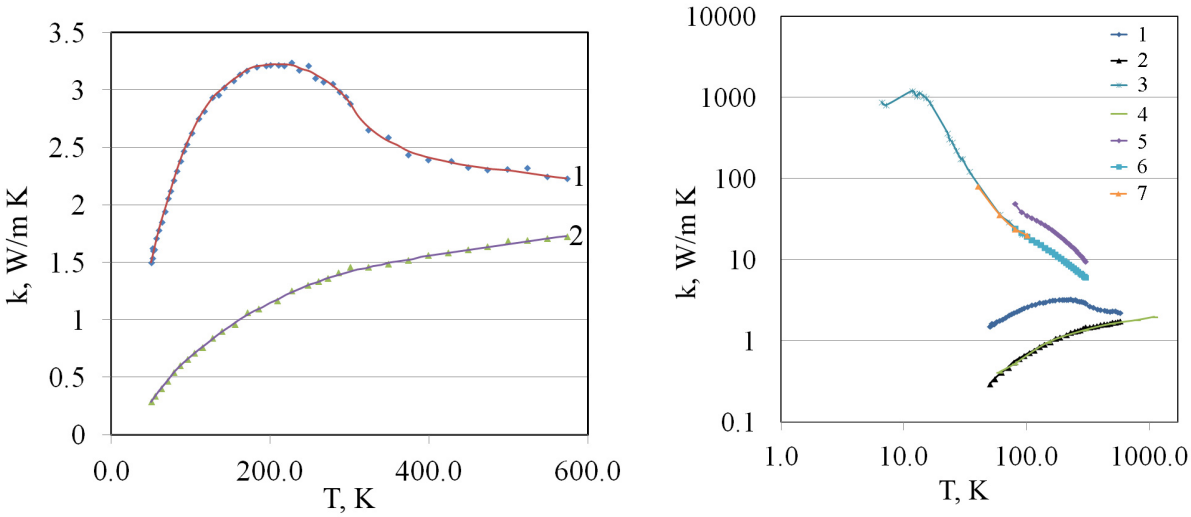

FIG. 6. Thermal conductivity of flintstone (our measurements) (1), quartz glass (our measurements) (2), quartz single crystal [25] (3), quartz glass [26] (4), quartz single crystal [27] (measured parallel to quartz optical axis) (5), quartz single crystal [27] (measured perpendicularly to quartz optical axis) (6), quartz single crystal [28] (7)

Thus, said chalcedony grains are the aggregates of very thin fibers that are invisible in optical microscope (their size indicates their colloidal nature); these fibers are allocated in the orderly, subparallel manner, i.e., in a radial pattern" [19]. However, our data amend the above observation with novel nano-level atomic force microscopy results.

The studied natural flintstone samples have a similar structure with laboratory-synthesized compacts of various chemical compositions prepared as nanopowders [11] as per the aforementioned atomic force microscopy in combination with X-ray phase analysis results, also confirming said hierarchic structure. Optical transmittance spectrum of flintstone has shown the unequivocal presence of water/hydroxyl moieties; but said water content in flintstone is essentially less than observed ca. 1 wt.% mass loss under heating, for such weight change corresponds to elimination of both water and elementary carbon. Also, it is worth mentioning that natural flintstone's hardness is higher than that of laboratory-synthesized compacts due to the different ripening time of these artificial and natural materials.

In addition, the studied flintstone specimens were nano-mineralogy objects [30] and, in general, black flintstones, exhibiting efficient luminescence, belong to nano-photonics.

Acknowledgement

The authors express their appreciation to V. Kuzin and E.M. Spiridonov for their optical treatment of the samples and to E.M. Spiridonov, A. M. Generalov and S. V. Kuznetsov for their discussion of the results.

This work was performed as a part of research plan of General Physics Institute. Some measurements were done in the Collective Use Centers of General Physics Institute and Institute of General and Inorganic Chemistry of the Russian Academy of Sciences.

References

[1] *Diffraction Nanophotonics*. Ed. V. A. Soifer. Moscow, Fizmatlit, 2011, 680 p. (in Russian).
[2] *Optical properties of photonic structures: interplay of order and disorder*. Ed. M.F. Limonov, R.M. De La Rue. Boca Raton, CRC/Taylor& Francis Group, 2012, XVII, 514 pp.
[3] Wiersma D. The smallest random laser. *Nature*, 2000, **406,** P. 132–133.
[4] García P.D., Sapienza R., Lo'pez C. Photonic Glasses: A Step Beyond White Paint. *Adv. Mater.*, 2010, **22**, P. 12–19.
[5] Barthelemy P., Bertolotti J., Wiersma D.S. A Le'vy flight for light. *Nature*, 2008, **453**, P. 495–498.
[6] Kouznetzov S.V., Yarotskya I.V., Fedorov P.P., Voronov V.V., Lavristchev S.V., Basiev T.T., Osiko V.V. Preparation of nanopowdered $M_{1-x}R_xF_{2+x}$ (M = Ca, Sr, Ba; R = Ce, Nd, Er, Yb) solid solutions. *Rus. J. Inorg. Chem*., 2007, **52**, P. 315–320.
[7] Fedorov P.P., Tkatchenko E.A., Kouznetzov S.V., Voronov V.V., Lavristchev S.V. Preparation of MgO nanoparticles. *Inorg. Mater*., 2007, **43**, **5**, P. 502-504.
[8] Kuznetsov S.V., Fedorov P.P., Voronov V.V., Samarina K.S., Ermakov R.P., Osiko V.V. Synthesis of $Ba_4R_3F_{17}$ (R stands for rare earth elements) powders and transparent compacts on their base. *Rus. J. Inorg. Chem.*, 2010, **55**(4), P. 484–493.
[9] Kuznetsov S.V., Fedorov P.P., Voronov V.V., Osiko V.V. Synthesis of $MgAl_2O_4$ Nanopowders. *Inorg. Mater.*, 2011, **47**, P. 895–898.
[10] Fedorov P.P., Kuznetsov S.V., Mayakova M.N., Voronov V.V., Ermakov R.P., Baranchikov A.E., Osiko V.V. Coprecipitation from aqueous solutions to prepare binary fluorides. *Rus. J. Inorg. Chem*., 2011, **56**(10), P. 1525–1531.
[11] Mayakova M.N., Kuznetsov S.V., Fedorov P.P., Voronov V.V., Ermakov R.P., Boldyrev K.N., Karban' O.V., Uvarov O.V., Baranchikov A.E., Osiko V.V. Synthesis and characterization of fluoride xerogels. *Inorg. Mater.*, 2013, **49**, **11**, P. 1152–1156.
[12] Mayakova M.N., Luginina A.A., Kuznetsov S.V., Voronov V.V., Ermakov R.P., Baranchikov A.E., Ivanov V.K., Karban' O.V., Fedorov P.P. Synthesis of SrF_2-YF_3 nanopowders by co-precipitation from aqueos solutions. *Mendeleev Commun.*, 2014, **24**(6), P. 360–362.
[13] Niederberger M., Colfen H. Oriented attachment and mesocrystals: Non-classical crystallization mechanisms based on nanoparticle assembly. *PhysChemChemPhys*, 2006, **8**, P. 3271–3287.
[14] Fedorov P.P., Ivanov V.K. Cooperative formation of crystals by aggregation and intergrowth of nanoparticles. *Dokl. Phys.*, 2011, **56**(4), P. 205–207.
[15] Ivanov V.K., Fedorov P.P., Baranchikov A.Y., Osiko V.V. Oriented aggregation of particles: 100 years of investigations of non-classical crystal growth. *Russ. Chem. Rev.*, 2014, **83**(12), P. 1204–1222.
[16] Smol'yaninov N.A. *Practical guide to mineralogy*. Moscow, Nedra, 1955, 432 p.
[17] Godovikov A.A., Ripinen O.I., Motorin S.G. *Agates*. Moscow, Nedra, 1987, 368 p (in Russian).
[18] Zdorik T.B. Opal. *Priroda*, 1990, **10**, P. 40–43 (in Russian).
[19] Frolov V.T. *Lithology*. Book 1. Moscow, Lomonosov St.Univ., 1992, 336 p. (in Russian).
[20] Spiridonov E.M., Ladygin V.M., Yanakieva D.Ya., Frolova Yu.V., Semikolennyh E.S. Agates in metavolcanics. Geological conditions, parameters and time of transformation of volcanites into mandelites with agates. Ed. Panchenko V.Ya. "MOLNET" Special issue of the magazine "Herald of RFBR", Moscow, 2014, 72 p. (in Russian).
[21] Popov P.A., Sidorov A.A., Kul'chenkov E.A., Anishchenko A.M., Avetissov I.Ch., Sorokin N.I., Fedorov P.P. Thermal conductivity and expansion of PbF_2 single crystals. *Ionics*, 2017, **23**, **1**, P. 233–239.
[22] Anderson J. H., Wickersheim K. A. Near infrared characterization of water and hydroxyl groups on silica surfaces. *Surface science*, 1964, **2**, P. 252–260.
[23] Ferrari A.C., Meyer J.C., Scardaci V., Casiraghi C., Lazzeri M., Mauri F., Piscanec S., Jiang D., Novoselov K.S., Roth S., Geim A.K. Raman spectrum of graphene and graphene layers. *Phys. Rev. Lett*., 2006, **97**, P. 18740.
[24] Khomich A.A., Kudryavtsev O.S., Dolenko T.A., Shiryaev A.A., Fisenko A.V., Konov V.I., Vlasov I.I. Anomalous enhancement of nanodiamond luminescence upon heating. *Laser Phys. Lett.*, 2017, **14**, P. 025702.
[25] Berman R. The thermal conductivities of some dielectric solids. *Proc. R. Soc. Lond. A*, 1951, **208**, P. 90–108.
[26] Sergeev O.A., Shashkov A.G., Umanskii A.S. Thermophysical properties of quartz glass. *J. Eng. Phys.*, 1982, **43**(6), P. 1375–1383.
[27] Novitsky L.A., Kozhevnikov I.G. *The thermophysical properties of materials at low temperatures (handbook)*. Mashinostroenie, Moscow, 1975 (in Russian).
[28] *Thermal Conductivity of Solids. Reference Book*. Ed. by A.S. Okhotin. Moscow, Energoatomizdat, 1984 (Russian).
[29] Popov P.A., Fedorov P.P., Kuznetsov S.V., Konyushkin V.A., Osiko V.V., Basiev T.T. Thermal conductivity of single crystals of $Ca_{1-x}Yb_xF_{2+x}$ solid solutions. *Dokl. Phys*., 2008, **53**(4), P. 198–200.
[30] Sedletskiy I.D. *Colloidal-dispersed mineralogy*. Ed. A.E. Fersman. Moscow, Leningrad, Academy of Science of the USSR, 1945, 114 p. (in Russian).
[31] Yushkin N.P., Askhabov A.M. et. al. *Nanomineralogy. Ultra- and micro-dispersed state of mineral matter*. St. Petersburg, Nauka, 2005, 581 p. (in Russian).